

Article

Can Energy Depletion of Wild Atlantic Salmon Kelts Negotiating Hydropower Facilities Lead to Reduced Survival?

Henrik Baktoft ^{1,*}, Karl Ø. Gjelland ², Marcell Szabo-Meszaros ^{3,4}, Ana T. Silva ⁵, Milan Riha ⁶, Finn Økland ⁵, Knut Alfredsen ⁴ and Torbjørn Forseth ⁵

¹ National Institute of Aquatic Resources, Technical University of Denmark (DTU Aqua), 8600 Silkeborg, Denmark

² Norwegian Institute of Nature Research (NINA), 9296 Tromsø, Norway; karl.gjelland@nina.no

³ SINTEF Energy Research, 7034 Trondheim, Norway; Marcell.Szabo-Meszaros@sintef.no

⁴ Department of Civil and Environmental Engineering, Norwegian University of Science and Technology, 7034 Trondheim, Norway; knut.alfredsen@ntnu.no

⁵ Norwegian Institute for Nature Research (NINA), 7034 Trondheim, Norway; Ana.Silva@nina.no (A.T.S.); Finn.Okland@nina.no (F.Ø.); Torbjorn.Forseth@nina.no (T.F.)

⁶ Biology Centre of the Czech Academy of Sciences, Institute of Hydrobiology, 370 05 České Budějovice, Czech Republic; mriha00@gmail.com

* Correspondence: hba@aqua.dtu.dk

Received: 2 July 2020; Accepted: 27 August 2020; Published: 7 September 2020

Abstract: Repeat spawners constitute an important component of Atlantic salmon populations, but survival of post-spawning individuals (kelts) are often compromised by anthropogenic structures such as hydropower plants (HPPs). Potential effects of HPPs include migration delays and associated increased energy depletion, which potentially results in increased overall mortality. We combined a detailed 3D hydraulic model with high-resolution 3D tracking of tagged kelts (length 73–104 cm) to obtain estimates of kelt movement through water. These estimates were then used in an energetics model to estimate hourly energy expenditure while negotiating the HPP area. Hourly kelt energy expenditure varied between 0.8 and 10.1 kJ × h⁻¹ and was dependent on kelt length. Degree of additional energy depletion can amount to several percent of remaining energy content (our study indicates 4–5 percentage points) potentially leading to reduced post-spawning survival. In turn, this can nullify the iteroparous breeding strategy and jeopardize long-term stability and persistence of Atlantic salmon populations inhabiting HPP rivers.

Keywords: high-resolution 3D telemetry; 3D hydraulic modeling; anthropogenic structures; river connectivity; energetics model; energy expenditure

1. Introduction

In Atlantic salmon (*Salmo salar*) populations, repeat spawners may make up a variable, but significant proportion of the total spawning fish biomass and egg deposition [1–3]. Repeat spawners are generally larger and more experienced than maiden spawners, which translates into comparatively higher fecundity [4,5] and thus, a larger contribution per capita to population growth. Modeling studies have shown that repeat spawners may have an important buffering and stabilizing effect on Atlantic salmon populations [6] and that kelt (i.e., post-spawning salmon) survival can be a significant factor for long-term population persistence [7].

Despite the large energy demands entailed by upstream migration and spawning, Atlantic salmon generally do not feed during this phase of their spawning migration (e.g., [8]). Post-spawning, Atlantic salmon kelts can resume some feeding whilst in-river [9], but given the size of available prey items relative to kelt size in most salmon rivers, their ability to restore their energy reserves before returning to sea is very low. Therefore, post-spawning, kelts are energetically depleted [10], and need to return to sea for foraging in order to survive and return as repeat spawners. A study indicated that even slight increases in overall depletion of energy reserves leads to highly increased mortality of these kelts [11]. Therefore, unobstructed river connectivity from spawning areas to the ocean is crucial for survival of the individual kelt and potentially for long-term persistence of local populations as increased mortality can compromise the bet-hedging breeding strategy leaving the population vulnerable to seasons with reproductive failure.

Many salmon rivers are affected by anthropogenic constructions, such as hydropower plants (HPPs) and associated structures (e.g., intake, dam and impounded river stretches) that inherently alter natural conditions and interrupt river connectivity. These structures may constitute barriers to both up- and downstream migration, and hamper or completely block passage for shorter or longer periods [12–16]. Such structures can be detrimental to salmon kelt survival both directly and indirectly [17]. During downstream migration, kelts can go through the turbines causing severe cuts and lesions and ultimately death. Additionally, visual observations of energy-depleted kelts entrained on trash racks or struggling to maintain body equilibrium and fight the current in front of trash racks at turbine intakes are common. However, little is known about kelt behavior in the impounded areas of the river, where directional current is more or less obliterated and the hydraulic conditions resemble a lake rather than a river. In these areas, salmon kelt (as well as other lotic fish species) can get disoriented and unable to negotiate the area and locate the bypass due to lack of current based directional guiding, thereby delaying their onward migration. Such delays might result in additional energy depletion of the kelts before they can reach the ocean and resume feeding, which in turn can be fatal for the individual kelt and thus stability of the local population. Besides the basic metabolism, the kelts might spend an excess amount of energy if they are actively searching for a passage opportunity. Delays in migration caused by HPP facilities have been associated with reduced passage success [17], and may be a significant factor for kelt survival.

Whereas overall survival, delay duration and passage routes of salmonid kelts negotiating hydropower facilities have previously been studied [17–19], knowledge of detailed kelt behavior and thus activity based energy expenditure is scarce or non-existing. Such knowledge is crucial to fully understand the impact of anthropogenic fragmentation of rivers. Knowledge of kelt behavior is also important to facilitate scientific based advice on, for example, design and operation of hydropower facilities, in particular on water intake area, bypass options and bypass flow regime.

In this study, we aimed at quantifying activity-based energy expenditure of kelt upstream of the Bjørset dam in a regulated river (the River Orkla, Norway) and relating it to the overall energetic status of the kelts. This was achieved by combining high-resolution 3D telemetry tracking of kelts, an energetic model including swimming speed, and a detailed 3D hydraulic model of the study area. This multi-disciplinary approach allowed us to estimate kelt energy expenditure based on detailed movement trajectories while accounting for effects of water flow direction and velocity.

2. Materials and Methods

2.1. Study Site

The study was carried out on the River Orkla in Central Norway (63°03' N, 9°40' E), which is designated as a national Norwegian salmon river. The mean annual discharge is ca. 72 m³s⁻¹. River connectivity is fragmented by several HPPs, however fish have particular difficulties negotiating the lowermost intake where water is directed to the Svorkmo HPP. The impounded section is controlled by the Bjørset dam located 100 m downstream of the Svorkmo intake tunnel. The dam consists of four spillway gates controlling the overall river flow regime at the site. One of these is open from May 1st each year to release a minimum flow following operational legislations. Additionally, the

dam contains two fish ladders, positioned at the northern and southern end of the dam. During winter, all spillway gates are closed and only $4 \text{ m}^3\text{s}^{-1}$ water is released downstream through the northern fish ladder. Water withdrawal towards the HPP typically varies between 20 and $55 \text{ m}^3\text{s}^{-1}$ through the intake tunnel. Entrance to the intake area is covered by an offset concrete wall with two submerged openings ($1.5 \text{ m} \times 25.8 \text{ m}$ each; approximately 2.2 m below the surface), constructed to prevent ice, debris and salmonid smolts from entering the HPP. Immediately in front of the intake, a trash rack is installed. See Szabo-Meszaros et al. (2019) [16] for further details on the study site.

2.2. Fish Tagging and Tracking

An array of 24 autonomous acoustic receivers (WHS3250, 76 kHz, Lotek Wireless Inc., Newmarket, ON, Canada) were deployed to enable high-resolution 3D tracking of tagged kelts (Figure 1). All receivers were kept at fixed positions by either mounting them to solid structures such as concrete walls or attaching them to weighted cross-like structures placed on the river floor. Receivers were positioned using a GNSS receiver (Trimble Geo7x) with a VRS-service providing 2 cm accuracy (CPOS-service from the Norwegian Mapping Authority). To allow for post-process synchronization of the receiver array, each receiver emitted a uniquely identifiable signal every 45 s using an internal transmitter. The receiver array was functional from 16 April 2016 to 1 June 2016.

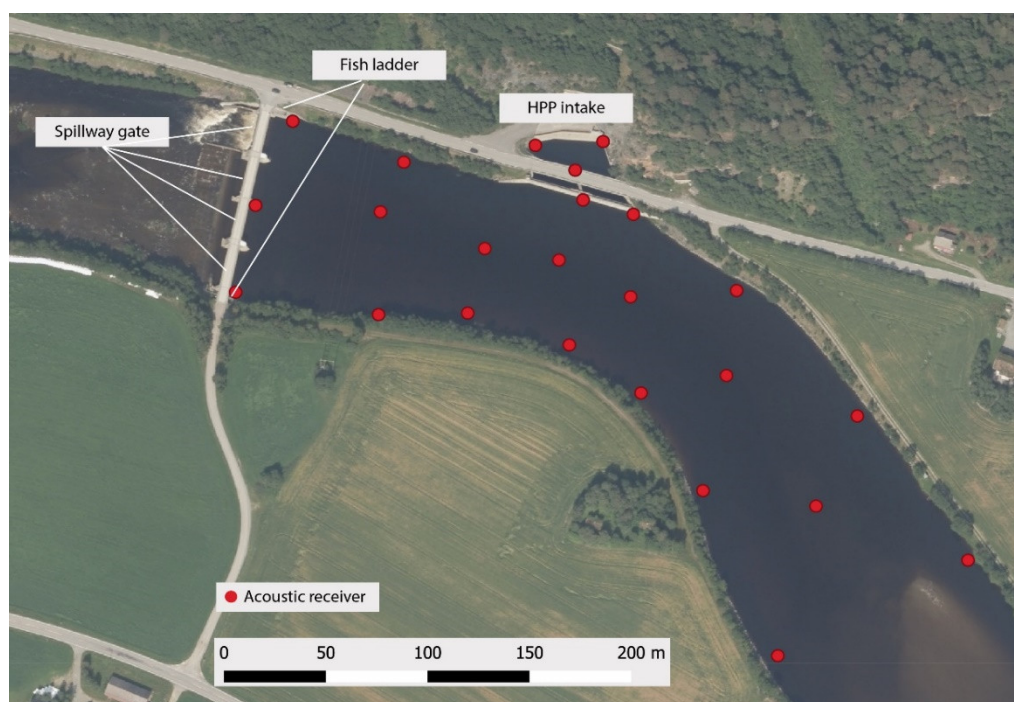


Figure 1. Overview of the study area. Aerial photo, Kartverket, Norway.

Fifty Atlantic salmon kelts were caught by local anglers using rod and reel during April 2016 at the study site ($N = 16$) or on the river stretches 0.8–10.5 km upstream ($N = 34$). Upon capture, each kelt was anesthetized (0.7 mL 2-phenoxyethanol per liter water, mean time in anesthetic bath 2 min 12 s), length measured to nearest centimeter and mass measured to nearest 0.1 kg. An acoustic transmitter with on-board pressure sensor (Lotek MM-M-11-28-PM (76 kHz), $12 \times 65 \text{ mm}$, 5.6 g in water, Lotek Wireless Inc., Newmarket, Ontario, Canada) was inserted into the body cavity through an incision. The incision was closed using two sutures (Ethicon Perma-hand, 5-0/FS-2). During surgery, kelts were kept in an anesthetics maintenance flow at half concentration (i.e., 0.35 mL 2-phenoxyethanol per liter water). The kelts were allowed to recover fully before being released back into the river. All tagged kelts were released at the same location they were caught. All handling and tagging were conducted according to the Norwegian regulations for treatment and welfare of animals (FOTS ID 8406).

Movement trajectories of tagged kelts were estimated based on detections by the receivers using the framework of Yet Another Positioning Solver [20] implemented in R package YAPS following the procedure outlined in Baktoft et al. (2019) [21]. YAPS has been shown to perform very well in acoustically challenging environments such as HPP intake areas [20,22]. Kelts were not necessarily detected continuously in the study area as they could utilize the upstream stretches of the river beyond receiver detection ranges and they could pass the area in downstream direction through the fish ladder to continue their migration. In situations where the kelts moved upstream of the receiver array, the estimated trajectories were fragmented.

2.3. Hydraulic Modelling

Simulations of the complex flow environment were performed using OpenFoam [23] computational fluid dynamics (CFD) on a digital model of the study site. The digital model extended to approximately 700 m upstream of the Bjørset dam and was bounded by the river bottom and by the hydropower structures (intake channel and dam with spillway gates and fish ladder). For detailed information about the hydraulic modeling approach and setup, see Szabo-Meszaros et al. (2019) [16].

Four different scenarios were selected to represent the temporal changes in water flow regime at the study site (Figures 2 and 3; Table 1). Specification and selection of the four scenarios was based on two prioritized parameters: the number of tagged kelts present in the area and the dam operation scheme (discharge through the HPP versus discharge through the spillway gates and fish ladder). Scenario I represents late winter conditions, when a majority of the river discharge was diverted to the HPP and only $4.0 \text{ m}^3\text{s}^{-1}$ was allowed through the fish ladder. Scenarios II and III represent a sudden change in both river discharge and dam operation in two steps as by 1st of May at least one gate was opened to release minimum discharge over the dam following local regulations. Scenario IV represents a situation characterized by high river discharge and a comparable amount of water going through the HPP and through the spillways ($Q_{\text{dam}}/Q_{\text{tunnel}} = 0.85$). Combined, these four scenarios cover the hydraulic conditions for 95% of the total time tagged kelts spent at the study site during the study period.

Table 1. Discharge characteristics of the four scenarios.

Scenario	Discharges (Q , m^3s^{-1})			Dam:Tunnel	
	Dam	Tunnel	Fish Ladder	Total	Ratio
I	0.0	22.4	4.0	26.3	0.00
II	8.0	28.8	4.0	40.9	0.28
III	22.3	38.6	4.0	64.8	0.58
IV	38.4	45.4	0.5	84.3	0.85

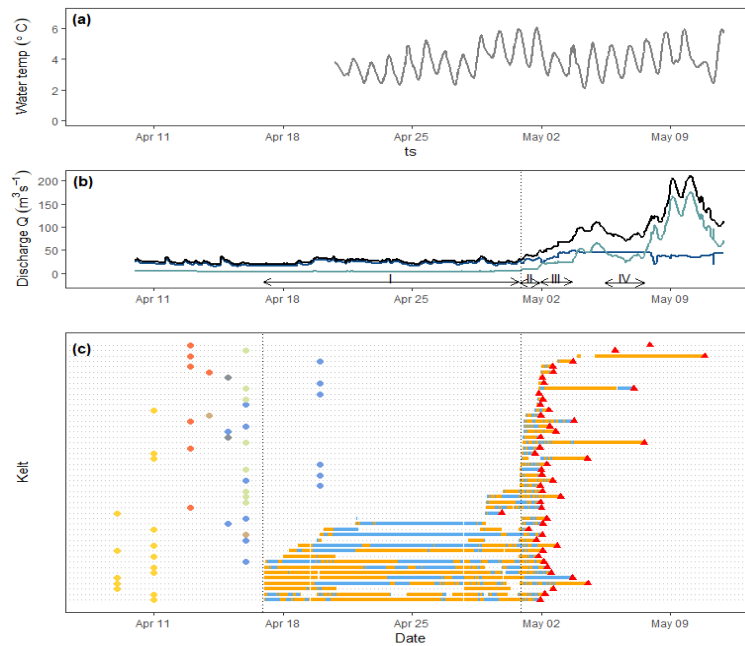


Figure 2. Water temperature (a), flow regimes and scenarios used in the hydraulic simulations (b) and overview of tracking periods for each individual kelt (c). Discharges are given over the dam (green), through the turbines (blue) and total (gray). Horizontal arrows and lines connecting them indicate periods represented by hydraulic scenarios I, II, III and IV. First partial opening of the spillway gates on May 1st is highlighted by dotted vertical line. Dots in (c) indicate time of tagging; color indicate tagging sites at following distances from the dam yellow: 0 km, blue: 1.8 km, green: 2.6 km, gray: 4.3 km, brown: 5.7 km, red: 10.5 km. Horizontal bars indicate periods in which individual kelt were tracked by the positioning system and either outside the hydraulic modeled area (orange) or inside the hydraulic modeled area (blue). Red triangles indicate time of last observation, i.e., the time kelt passed the dam. First partial opening of spillway gates on May 1st is highlighted by dotted vertical line. The tracking system was operational from midnight 16 April 2016 (first dotted vertical line) through midnight 1 June 2016.

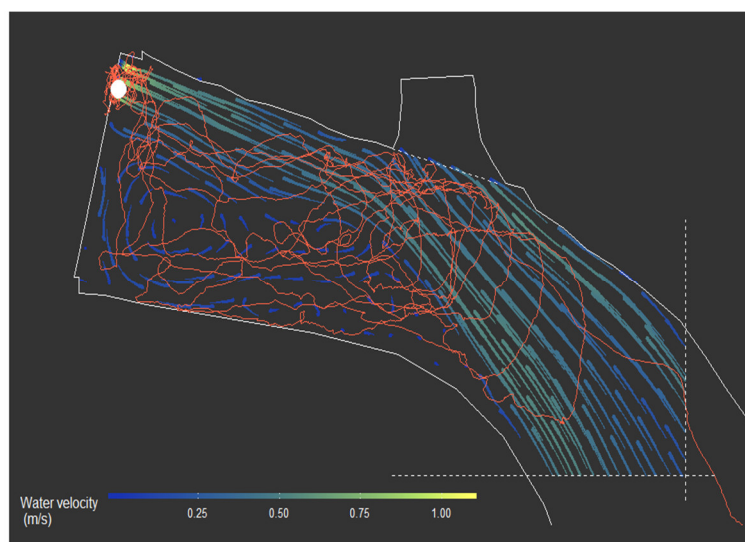


Figure 3. Example of simulated flow field in the study area (scenario III is shown). Colors indicate resultant water velocity in m s^{-1} and streamlines indicate flow direction. Broken white lines delimit the area covered by the hydraulic model. Example of movement trajectory of a single tagged kelt is included (red). This particular kelt spent 22 h negotiating the hydropower facility before leaving the area through spillway gate 1 on 1st May when the gate was lowered (white dot shows last estimated position).

For each of the four scenarios, water velocity vectors were sampled from the hydraulic model simulations on a predefined grid with 1×1 m resolution in the horizontal plane at multiple depths with 0.25 m intervals below the surface. Using these grids, each position in the estimated kelt tracks was assigned the temporally relevant water velocity vectors corresponding to the 3D fish position.

Simulations of the hydraulic model were carried out using the `pimpleFoam` utility of the `OpenFOAM` software for CFD applications [23].

2.4. Energetic Models

To enable quantification of movement based energy expenditure, we used already established equations for temperature and movement specific oxygen consumption in adult Atlantic salmon to construct a single unified model describing oxygen consumption as a function of water temperature, fish size and swimming speed. Using six separate equations for specific Atlantic salmon sizes (63.5 cm, 89.0 cm and 119.0 cm) and swimming speeds (0 bl s^{-1} , 0.5 bl s^{-1} , 0.7 bl s^{-1} and 1.0 bl s^{-1}) presented in Lennox et al. (2018) [24], we created an artificial data set covering relevant ranges of water temperature ($0\text{--}20$ °C), fish sizes (63.5–119.0 cm) and swimming speeds ($0\text{--}1 \text{ bl s}^{-1}$). Based on this data set, we developed the following model through an iterative model selection process:

$$\text{MO}_2 \sim N(\mu, \sigma^2) \quad (1)$$

$$\mu = \exp(-0.39 + 0.05 \times T + 0.0002 \times T^2 + 1.38 \times BLs + 0.28 \times BLs^2 - 0.038 \times L_T - 0.002 \times T \times BLs) \quad (2)$$

This model assumes that oxygen consumption (MO_2 ; unit $\text{mgO}_2 \text{ kg}^{-1} \text{ min}^{-1}$) is normally distributed with mean μ and variance σ^2 . Furthermore, the model states that the expected oxygen consumption of a kelt with total body length L_T , swimming at a speed of BLs body lengths per second in water with a temperature of T degrees Celsius is given by the predictor function μ . Oxygen consumption estimates obtained using our unified model correspond very well to estimates based on the original six separate equations established in Lennox et al. (2018) [24] (Pearson correlation: 0.98). The model was developed in a Bayesian framework using JAGS [25] and the R package R2jags [26]. Uninformative priors were used for all estimated parameters. Three chains of 100,000 iterations, thinning rate of 10 and a burn-in of 10,000 were used. All chains showed good mixing. See Supplementary Material S1 for additional details.

To enable quantification of the energy consumption relative to total kelt energy content, length dependent total energy content of the tagged kelts pre- and post-spawning were estimated using equations established in Jonsson, Jonsson and Hansen (1997) [11]. Specifically, Jonsson, Jonsson and Hansen (1997) [11] found that pre-spawning total energy content ($E_{T,\text{pre-spawn}}$; kJ) of Norwegian Atlantic salmon could be estimated from body length as:

$$E_{T,\text{pre-spawn}} = \exp(0.044 \times L_T + 6.99) \quad (3)$$

Similarly, we used the following equation from Jonsson, Jonsson and Hansen (1997) [11] to obtain estimates of post-spawning total energy content ($E_{T,\text{post-spawn}}$; kJ):

$$E_{T,\text{post-spawn}} = \exp(0.035 \times L_T + 6.51) \quad (4)$$

2.5. Hourly Energy Expenditure

To allow estimation of kelt movement through water, only estimated kelt positions within coverage of the hydraulic model were included in analyses of hourly energy expenditure. Furthermore, kelt movement trajectories were split into 10 min sequences and only sequences where at least 95% of all potential positions were available and within coverage of the hydraulic model were included in the analyses. Within each 10 min trajectory sequence, we estimated instantaneous 2D kelt over ground swimming speed vector components (ΔX_{og} ; ΔY_{og}) for each position (except the last in each sequence) as:

$$(\Delta X_{og,n}; \Delta Y_{og,n}) = ((X_{n+1} - X_n)/(ToP_{n+1} - ToP_n); (Y_{n+1} - Y_n)/(ToP_{n+1} - ToP_n)) \quad (5)$$

In which X and Y are estimated kelt positions and ToP is the estimated time of ping, in other words, time of signal transmission. Using these, we estimated 2D kelt movement speed through water by accounting for water velocity as:

$$V_{tw,n} = ((\Delta X_{og,n} - u_s)^2 + (\Delta Y_{og,n} - v_s)^2)^{1/2} \quad (6)$$

In which u_s and v_s are the flow velocity components in x and y , respectively, obtained from the hydraulic model for the temporally relevant scenario s . Subsequently, instantaneous movement speed through water measured as body lengths per second (BL_{Stw}) was calculated by dividing by kelt total length L_T :

$$BL_{Stw} = V_{tw} \times L_T^{-1} \quad (7)$$

Values for BL_{Stw} were then used in our model for oxygen consumption to obtain instantaneous oxygen consumption ($MO_{2,n}$) for each estimated position. To avoid extrapolating beyond the maximum swimming speed used to construct our unified energy consumption model, values of BL_{Stw} higher than 1 bl s^{-1} were truncated to 1 bl s^{-1} . However, kelt were rarely observed swimming at speeds above 1 bl s^{-1} (<1% of observations). Based on these individual and sequence specific values for oxygen consumption, we then calculated expected average hourly energy consumption for each ten minute sequence as:

$$E_{\text{mean, hour}} = 60 \times \sum(MO_{2,i} \times W_{\text{kelt}} \times 0.0136) \times n^{-1}, \text{ for } i \text{ in } [1; n - 1] \quad (8)$$

where W_{kelt} is mass of the kelt (in kilograms) at time of tagging. The constant is a factor converting oxygen consumption to energy in kilojoules based on the caloric conversion factor used in Lennox et al. (2018) [24]. Finally, n is total number of observations in each sequence. Thus, for all 10 min trajectory sequences included in this analysis, we obtained an estimate of average energy consumption per hour. To generalize this to a kelt length specific population level estimate of energy consumption, we used the following simple linear mixed effect model:

$$E_{\text{mean, hour}} \sim N(\mu_E, \sigma_E^2 \times \exp(2 \times \delta \times L_T)) \quad (9)$$

$$\mu_E = \alpha + L_T + a_{\text{kelt}} \quad (10)$$

$$a_{\text{kelt}} \sim N(0, \sigma_a^2) \quad (11)$$

This model assumes that the expected mean energy consumption per hour ($E_{\text{mean, hour}}$) is normally distributed with mean μ_E and an exponential variance structure ($\sigma_E^2 \times \exp(2 \times \delta \times L_T)$) modeling variance of the residuals as a function of kelt total length (L_T), thereby allowing heterogeneity in the residuals. Parameters σ_E and δ are estimated. This variance structure was included as preliminary analyses suggested that heterogeneity of model residuals increased as a function of kelt total length. Furthermore, comparison of AIC (Akaike information criterion) values for models with and without the exponential variance structure clearly supported inclusion ($\Delta AIC = -129$). The linear predictor function (μ_E) is defined as the sum of a common intercept (α), an effect of kelt total length (L_T) modeled as a continuous covariate and kelt is modeled as a random effect with mean zero and variance σ_a^2 to account for repeated measures on each kelt. This model was fitted using the R package nlme [27]. Model assumptions were validated using visual inspection of model residuals following Zuur et al. (2009) [28].

To quantify the effect of increased energy expenditure caused by HPP-induced migration delays on total kelt energy reserves, we related the cumulative effect of predicted hourly energy expenditure for $t = [1; 30]$ days to expected pre-spawning total energy reserves as:

$$E_{\text{rel, remaining}} = 1 - (E_{T,\text{pre-spawn}} - E_{\text{mean, hour}} \times t \times 24) / E_{T,\text{pre-spawn}} \quad (12)$$

Estimation of kelt movement trajectories and all statistical analyses were performed in R [29].

3. Results

Tracks were obtained from 48 of the 50 tagged kelts (example in Figure 3). Individual kelt track duration varied considerably as some kelts remained within the surveyed area the entire study period, whereas others moved upstream and thus resided outside hydrophone detection range for extended periods. No mortality of tagged kelt were observed within the study area. All 48 tracked kelts left the study area by going either through the fish ladder or through the spillway gates, evidenced by their tracks ending at or in close proximity to the dam. Additionally, one kelt left the study area before the tracking system was fully operational.

In total, ca. 7.8 million kelt positions were estimated of which 3.3 million (42%) were inside the area and period covered by the hydraulic model. Of these, 2.9 million (88%) were included in analyses of energy expenditure as at least 95% of the expected positions in each 10 min sequence were available.

Generally, kelt downstream migration was seemingly influenced by changes in river discharge and the operation scheme of the HPP. Entrance to the study area from upstream stretches coincided with increase in river discharge for a slight majority of the tagged kelts. Moreover, only two kelts were found to successfully pass the study area prior to opening the spillway gates on 1st May (Figure 2). The successful passage of one of these was documented by the tracking system; whereas the other is based on raw hydrophone detections in the early phases before the tracking system was completely operational (this kelt is not included in subsequent analyses).

Duration from tagging until leaving the study area ranged from approximately 11 to 28 days. The estimated energy expenditure per hour for the tagged kelts while inside the area covered by the hydraulic model, varied between 0.8 and 10.1 $\text{kJ} \times \text{h}^{-1}$ (minimum and maximum) and was dependent on kelt total length (Figure 4; linear mixed effect model: $p < 0.001$). Forecasting this hourly energy expenditure for up to 30 days results in relative remaining energy dropping by approximately 4 to 5 percentage points dependent on kelt length (Figure 5).

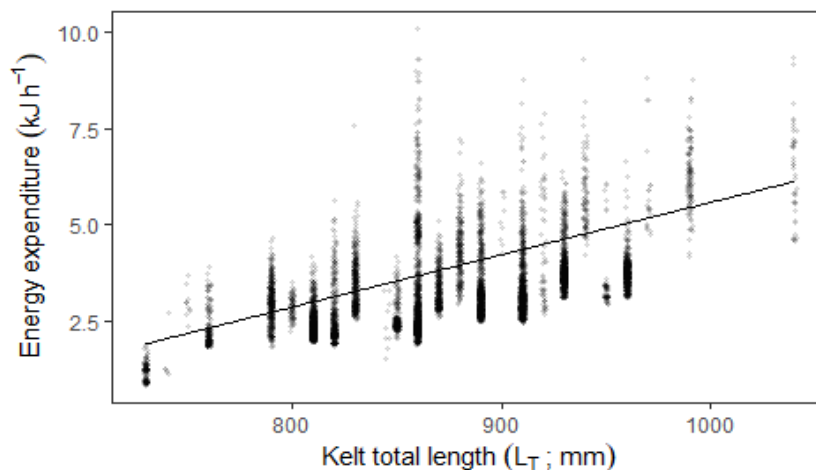


Figure 4. Energy expenditure per hour as function of kelt total length. Points show the estimated average energy expenditure per hour ($E_{\text{mean, hour}}$) based on kelt movement through water (jitter introduced to help visualization). The line shows marginal predictions from the mixed effect model, i.e., the expected length specific energy expenditure.

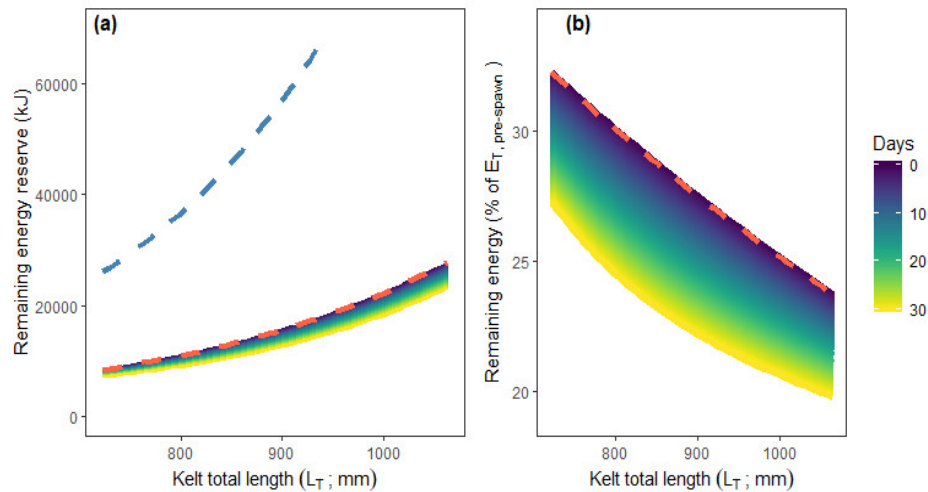


Figure 5. Kelts delayed in downstream migration experience gradual energy depletion. (a) Progressive energy depletion of Atlantic salmon kelts. Hatched lines represent pre-spawning (blue) and post-spawning (red) total energy content [9]. Blue-yellow gradient shows cumulative energy depletion per day spent in front of the HPP facility. (b) Cumulative depletion of remaining energy content relative to pre-spawning. Red hatched line represents post-spawning total energy content [11].

4. Discussion

Our study indicates that Atlantic salmon kelts can be exposed to substantial additional depletion of energy reserves if their successful passage of migration barriers (e.g., HPP dams and weirs) is delayed. In our study, only 2 out of 50 tagged kelts successfully negotiated the study area before one or more of the spillway gates were lowered allowing water to pass through. This suggests that the HPP operation scheme effectively controlled the kelt downstream migration and that the observed persistent presence of kelts in the study area and upstream sections indeed reflected a delay caused by the HPP. Although all tagged kelts appearing in the intake area finally successfully passed, the delay may have profound consequences for the remaining energy reserves and subsequent survival.

Forecasting the estimated hourly energy expenditure while negotiating the HPP facility to 30 days indicated that kelts will suffer additional energy depletion amounting to 4–5 percent of pre-spawning energy content compared to a no-delay scenario. Jonsson, Jonsson and Hansen (1997) [11] found that even minor additional energy depletion lead to considerable reduction in kelt post-spawning survival rates. Specifically, increasing energetic loss by 4 percentage points reduces the already low kelt survival rate by approximately 10 percentage points [11]. This is further corroborated by Nyqvist et al. (2016) [17] reporting that delays may result in reduced overall passage success.

Our study documents that the delay caused by HPPs does indeed have an energetic cost which ultimately can result in reduced kelt survival. Although outside the scope of the present study, we advocate the importance of knowledge based and flexible HPP operation schemes to allow efficient passage of kelts. Many salmon rivers are equipped with multiple HPPs positioned from high upstream to near the river mouth. In these rivers, delays caused by individual HPP facilities and associated increase in energy expenditure can be cumulative, further strengthening the need for proper HPP operation schemes.

Variation in river discharge and water temperature are important cues initiating and controlling salmonid migration [30,31]. At the study site, river discharge was to a large extent regulated by upstream HPP facilities effectively enshrouding the natural fluctuations. This may have influenced kelt migratory behavior as natural cues to initiate or continue downstream migration might have been obliterated. Such anthropogenic alterations of the river flow combined with influence of the dam at the study site makes it impossible to separate effects of natural variation

in river discharge and HPP operation scheme on kelt passage time and behavior. Additionally, it is impossible to predict what passage times of the focal river stretch would be under natural conditions. However, previous studies show that in-river downstream migration of post-spawned Atlantic salmon generally is relatively fast (median values of 3.7 km d⁻¹ and 9.3 km d⁻¹ reported in [9,17]) and that HPP dams can cause severe delays [17]. Furthermore, successful passage of HPP dams has previously been shown to predominantly occur through open spillway gates [17]. In our study, open spillway gates were not available until towards the end of the migration period. The fact that most kelts rapidly passed as soon as the gates opened is indeed a strong indication that the regulation management influenced migration behavior. Although the discharge was increasing at the same time, many kelts migrated at discharges also observed a couple of days earlier without such migration from the dam (see Figure 2). The alternative explanation that this rapid response was initiated by increasing discharge seems much more speculative. Therefore, we regard it as a fair assumption that the observed prolonged residence times at the focal river stretch were caused by the HPP structures and that given natural conditions in the River Orkla, residence time and associated energy consumption at the focal river stretch would be negligible in comparison to the observed delays.

Our estimates on energy expenditure are based on previously established models. Specifically, we used models on energy consumption of discrete body sizes, at discrete water temperatures and discrete activity levels [24] to obtain a unified continuous model accommodating the ranges of fish sizes, water temperatures and activity levels observed in this study. However, results in Lennox et al. (2018) [24] are based on farmed Atlantic salmon in good condition, while the salmon in our study were energy deprived Atlantic salmon kelt of wild origin. The implications of this on the estimates of energy expenditure are unknown, but Robertsen et al. (2019) [32] did not find conclusive evidence that farmed Atlantic salmon juveniles differ in standard metabolic rate from their wild counterparts. Additionally, maximum activity levels in Lennox et al. (2018) [24] were limited to swimming activities corresponding to one body length per second. While a majority of the tagged kelts (78%) occasionally were registered to swim faster than that, more than 99% of the registered swimming speeds were within range of the underlying model, in other words, between zero and one body length per second. Furthermore, any bias introduced by truncating the maximum swimming speed would result in more conservative (i.e., lower) estimates of energy expenditure. We acknowledge that our model-based approach potentially introduces uncertainties and biases. Optimally, measurements of energy expenditure should have been performed on the tracked kelts, but such activities were beyond the scope of the present study.

5. Conclusions

Our study documents that kelt energy reserves are depleted as kelts spend time negotiating anthropogenic structures. The degree of energy reserve depletion obviously depends on duration of time spent negotiating the structures, but can conceivably amount to several percent of total pre-spawning energy content, which ultimately can lead to reduced post-spawning survival. In turn, this can nullify the iteroparous breeding strategy and jeopardize long-term stability and persistence of local Atlantic salmon populations. To improve conservation status of Atlantic salmon in HPP rivers, we therefore advocate the need for knowledge based and flexible HPP operations schemes focused at enhancing opportunities for successful kelt downstream migration. Additionally, we advocate that future research focused on development of efficacious bypass solutions is needed to supplement HPP operations schemes to ensure best possible survival of migrating Atlantic salmon and other fishes.

Supplementary Materials: The following are available online at www.mdpi.com/2071-1050/12/18/7341/s1, energy model in R.

Author Contributions: Conceptualization, H.B., K.Ø.G., F.Ø. and T.F.; formal analysis, H.B., K.Ø.G., M.S.-M. and K.A.; funding acquisition, T.F.; methodology, H.B., K.Ø.G., M.S.-M., A.T.S., F.Ø. and K.A.; project administration, K.A. and T.F.; visualization, H.B., M.S.-M. and M.R.; writing—original draft, H.B., K.Ø.G.,

M.S.-M., A.T.S., M.R. and F.Ø.; writing—review and editing, H.B., K.Ø.G., M.S.-M., A.T.S., M.R., F.Ø., K.A. and T.F. All authors have read and agreed to the published version of the manuscript.

Funding: This research was supported by the SafePass project (project no. 244022) funded by the Research Council of Norway (RCN) under the ENERGIX program, 13 hydropower companies, the Norwegian Environment Agency and the Norwegian Water Resources and Energy Directorate. Additional funding was provided by the Norwegian Research Centre for Hydropower Technology—HydroCen (RCN project no. 257588).

Acknowledgments: The authors wish to thank Eva Ulvan and Ingebrigt Uglem for tagging of the kelts. Local fishermen are thanked for helping with catching the kelts. The simulations on HPC system were performed on resources provided by UNINETT Sigma 2, the National Infrastructure for High Performance Computing and Data Storage in Norway.

Conflicts of Interest: The authors declare no competing interest. The funders had no role in the design of the study; in the collection, analyses, or interpretation of data; in the writing of the manuscript, or in the decision to publish the results.

References

- Bordeleau, X.; Pardo, S.A.; Chaput, G.; April, J.; Dempson, B.; Robertson, M.; Levy, A.; Jones, R.; Hutchings, J.A.; Whoriskey, F.G.; et al. Spatio-temporal trends in the importance of iteroparity across Atlantic salmon populations of the northwest Atlantic. *ICES J. Mar. Sci.* **2020**, *77*, 326–344, doi:10.1093/icesjms/fsz188.
- Fleming, I.A. Pattern and variability in the breeding system of Atlantic salmon (*Salmo salar*), with comparisons to other salmonids. *Can. J. Fish. Aquat. Sci.* **1998**, *55*, 59–76, doi:10.1139/d98-009.
- Niemelä, E.; Orell, P.; Erkinaro, J.; Dempson, J.B.; Brørs, S.; Svenning, M.A.; Hassinen, E. Previously spawned Atlantic salmon ascend a large subarctic river earlier than their maiden counterparts. *J. Fish Biol.* **2006**, *69*, 1151–1163, doi:10.1111/j.1095-8649.2006.01190.x.
- De Gaudemar, B.; Bonzom, J.M.; Beall, E. Effects of courtship and relative mate size on sexual motivation in Atlantic salmon. *J. Fish Biol.* **2000**, *57*, 502–515, doi:10.1006/jfbi.2000.1331.
- Fleming, I.A. Reproductive strategies of Atlantic salmon: Ecology and evolution. *Rev. Fish Biol. Fish.* **1996**, *6*, 379–416, doi:10.1007/BF00164323.
- Halttunen, E. Staying alive—The survival and importance of Atlantic salmon post-spawners. Ph.D. Thesis, University of Tromsø, Tromsø, Norway, 2011.
- Lawrence, E.R.; Kuparinen, A.; Hutchings, J.A. Influence of dams on population persistence in Atlantic salmon (*Salmo salar*). *Can. J. Zool.* **2016**, *94*, 329–338, doi:10.1139/cjz-2015-0195.
- Kadri, S.; Metcalfe, N.B.; Huntingford, F.A.; Thorpe, J.E. What Controls the Onset of Anorexia in Maturing Adult Female Atlantic Salmon? *Funct. Ecol.* **1995**, *9*, 790–797, doi:10.2307/2390254.
- Huble, P.B.; Amiro, P.G.; Gibson, A.J.F.; Lacroix, G.L.; Redden, A.M. Survival and behaviour of migrating Atlantic salmon (*Salmo salar* L.) kelts in river, estuarine, and coastal habitat. *ICES J. Mar. Sci.* **2008**, *65*, 1626–1634, doi:10.1093/icesjms/fsn129.
- Jonsson, N.; Jonsson, B.; Hansen, L.P. Energetic cost of spawning in male and female Atlantic salmon (*Salmo salar* L.). *J. Fish Biol.* **1991**, *39*, 739–744, doi:10.1111/j.1095-8649.1991.tb04403.x.
- Jonsson, N.; Jonsson, B.; Hansen, L.P. Changes in Proximate Composition and Estimates of Energetic Costs During Upstream Migration and Spawning in Atlantic Salmon *Salmo salar*. *J. Anim. Ecol.* **1997**, *66*, 425, doi:10.2307/5987.
- Lucas, M.C.; Baras, E. *Migration of Freshwater Fishes*; Blackwell Science: Oxford, UK, 2001.
- Poff, N.L.; Allan, J.D.; Bain, M.B.; Karr, J.R.; Prestegard, K.L.; Richter, B.D.; Sparks, R.E.; Stromberg, J.C. The Natural Flow Regime. *Bioscience* **1997**, *47*, 769–784, doi:10.2307/1313099.
- Silva, A.T.; Lucas, M.C.; Castro-Santos, T.; Katopodis, C.; Baumgartner, L.J.; Thiem, J.D.; Aarestrup, K.; Pompeu, P.S.; O'Brien, G.C.; Braun, D.C.; et al. The future of fish passage science, engineering, and practice. *Fish Fish.* **2018**, *19*, 340–362, doi:10.1111/faf.12258.
- Silva, A.T.; Bærum, K.M.; Hedger, R.D.; Baktoft, H.; Fjeldstad, H.P.; Gjelland, K.; Økland, F.; Forseth, T. The effects of hydrodynamics on the three-dimensional downstream migratory movement of Atlantic salmon. *Sci. Total Environ.* **2020**, *705*, 135773, doi:10.1016/j.scitotenv.2019.135773.

16. Szabo-Meszaros, M.; Forseth, T.; Baktoft, H.; Fjeldstad, H.-P.; Silva, A.T.; Gjelland, K.Ø.; Økland, F.; Uglem, I.; Alfredsen, K. Modelling mitigation measures for smolt migration at dammed river sections. *Ecohydrology* **2019**, e2131, doi:10.1002/eco.2131.
17. Nyqvist, D.; Calles, O.; Bergman, E.; Hagelin, A.; Greenberg, L.A. Post-spawning survival and downstream passage of landlocked Atlantic salmon (*Salmo salar*) in a regulated river: Is there potential for repeat spawning? *River Res. Appl.* **2016**, *32*, 1008–1017, doi:10.1002/rra.2926.
18. Kraabøl, M.; Arnekleiv, J.V.; Museth, J. Emigration patterns among trout, *Salmo trutta* (L.), kelts and smolts through spillways in a hydroelectric dam. *Fish. Manag. Ecol.* **2008**, *15*, 417–423, doi:10.1111/j.1365-2400.2008.00633.x.
19. Nyqvist, D.; Bergman, E.; Calles, O.; Greenberg, L. Intake Approach and Dam Passage by Downstream-migrating Atlantic Salmon Kelts. *River Res. Appl.* **2017**, *33*, 697–706, doi:10.1002/rra.3133.
20. Baktoft, H.; Gjelland, K.Ø.; Økland, F.; Thygesen, U.H. Positioning of aquatic animals based on time-of-arrival and random walk models using YAPS (Yet Another Positioning Solver). *Sci. Rep.* **2017**, *7*, 14294, doi:10.1038/s41598-017-14278-z.
21. Baktoft, H.; Gjelland, K.Ø.; Økland, F.; Rehage, J.S.; Rodemann, J.R.; Corujo, R.S.; Viadero, N.; Thygesen, U.H. Opening the black box of high resolution fish tracking using yaps. *bioRxiv* **2019**, doi:10.1101/2019.12.16.877688.
22. Vergeynst, J.; Vanwyck, T.; Baeyens, R.; De Mulder, T.; Nopens, I.; Mouton, A.; Pauwels, I. Acoustic positioning in a reflective environment: Going beyond point-by-point algorithms. *Anim. Biotelemetry* **2020**, *1*–17, doi:10.1186/s40317-020-00203-1.
23. Greenshields, C. OpenFOAM Foundation Ltd. The Open Source CFD toolbox (v 4.1.0). 2015. Available online: <https://openfoam.org/> (accessed on 9 July 2020).
24. Lennox, R.J.; Eliason, E.J.; Havn, T.B.; Johansen, M.R.; Thorstad, E.B.; Cooke, S.J.; Diserud, O.H.; Whoriskey, F.G.; Farrell, A.P.; Uglem, I. Bioenergetic consequences of warming rivers to adult Atlantic salmon *Salmo salar* during their spawning migration. *Freshw. Biol.* **2018**, *63*, 1381–1393, doi:10.1111/fwb.13166.
25. Plummer, M. JAGS: A Program for Analysis of Bayesian Graphical Models Using Gibbs Sampling. In Proceedings of the 3rd International Workshop on Distributed Statistical Computing; Vienna, Austria, 20–22 March 2003.
26. Su, Y.-S.; Yajima, M. R2jags: Using R to Run “JAGS” R Package Version 0.6-1 2020. Available online: <https://CRAN.R-project.org/package=R2jags> (accessed on 9 July 2020).
27. Pinheiro, J.; Bates, D.; DebRoy, S.; Sarkar, D.; The R Core Team. nlme: Linear and Nonlinear Mixed Effects Models. R Package Version 3.1-144. 2020. Available online: <https://CRAN.R-project.org/package=nlme> (accessed on 9 July 2020).
28. Zuur, A.F.; Ieno, E.N.; Walker, N.J.; Saveliev, A.A.; Smith, G.M. *Mixed Effects Models and Extensions in Ecology with R*; Springer: New York, NY, USA, 2009.
29. R Core Team R: *A Language and Environment for Statistical Computing*; R Foundation for Statistical Computing: Vienna, Austria, 2020. Available online: <https://cran.r-project.org/> (accessed on 9 July 2020).
30. Banks, J.W. A Review of the Literature on the Upstream Migration of Adult Salmonids. *J. Fish Biol.* **1969**, *1*, 85–136, doi:10.1111/j.1095-8649.1969.tb03847.x.
31. Thorstad, E.B.; Økland, F.; Aarestrup, K.; Heggberget, T.G. Factors affecting the within-river spawning migration of Atlantic salmon, with emphasis on human impacts. *Rev. Fish Biol. Fish.* **2008**, *18*, 345–371, doi:10.1007/s11160-007-9076-4.
32. Robertsen, G.; Reid, D.; Einum, S.; Aronsen, T.; Fleming, I.A.; Sundt-Hansen, L.E.; Karlsson, S.; Kvingedal, E.; Ugedal, O.; Hindar, K. Can variation in standard metabolic rate explain context-dependent performance of farmed Atlantic salmon offspring? *Ecol. Evol.* **2019**, *9*, 212–222, doi:10.1002/ece3.4716.

